BMC Chemistry

RESEARCH ARTICLE

Open Access

# Construction of a novel quinoxaline as a new class of Nrf2 activator

Murugesh Kandasamy[1,4†], Kit-Kay Mak[1,2,4†], Thangaraj Devadoss[5*], Punniyakoti Veeraveedu Thanikachalam[6], Raghavendra Sakirolla[7], Hira Choudhury[3,4] and Mallikarjuna Rao Pichika[1,4*]

## Abstract

**Background:** The transcription factor Nuclear factor erythroid-2-related factor 2 (NRF2) and its principal repressive regulator, Kelch-like ECH-associated protein 1 (KEAP1), are perilous in the regulation of inflammation, as well as maintenance of homeostasis. Thus, NRF2 activation is involved in cytoprotection against many inflammatory disorders. *N*′-Nicotinoylquinoxaline-2-carbohdyrazide (NQC) was structurally designed by the combination of important pharmacophoric features of bioactive compounds reported in the literature.

**Methods:** NQC was synthesised and characterised using spectroscopic techniques. The compound was tested for its anti-inflammatory effect using Lipopolysaccharide from *Escherichia coli* (LPS*Ec*) induced inflammation in mouse macrophages (RAW 264.7 cells). The effect of NQC on inflammatory cytokines was measured using enzyme-linked immune sorbent assay (ELISA). The Nrf2 activity of the compound NQC was determined using 'Keap1:Nrf2 Inhibitor Screening Assay Kit'. To obtain the insights on NQC's activity on Nrf2, molecular docking studies were performed using Schrödinger suite. The metabolic stability of NQC was determined using mouse, rat and human microsomes.

**Results:** NQC was found to be non-toxic at the dose of 50 µM on RAW 264.7 cells. NQC showed potent anti-inflammatory effect in an in vitro model of LPS*Ec* stimulated murine macrophages (RAW 264.7 cells) with an $IC_{50}$ value 26.13 ± 1.17 µM. NQC dose-dependently down-regulated the pro-inflammatory cytokines [interleukin (IL)-1β (13.27 ± 2.37 µM), IL-6 (10.13 ± 0.58 µM) and tumor necrosis factor (TNF)-α] (14.41 ± 1.83 µM); and inflammatory mediator, prostaglandin $E_2$ ($PGE_2$) with $IC_{50}$ values, 15.23 ± 0.91 µM. Molecular docking studies confirmed the favourable binding of NQC at Kelch domain of Keap-1. It disrupts the Nrf2 interaction with kelch domain of keap 1 and its $IC_{50}$ value was 4.21 ± 0.89 µM. The metabolic stability studies of NQC in human, rat and mouse liver microsomes revealed that it is quite stable with half-life values; 63.30 ± 1.73, 52.23 ± 0.81, 24.55 ± 1.13 min; microsomal intrinsic clearance values; 1.14 ± 0.31, 1.39 ± 0.87 and 2.96 ± 0.34 µL/min/g liver; respectively. It is observed that rat has comparable metabolic profile with human, thus, rat could be used as an in vivo model for prediction of pharmacokinetics and metabolism profiles of NQC in human.

**Conclusion:** NQC is a new class of NRF2 activator with potent in vitro anti-inflammatory activity and good metabolic stability.

**Keywords:** *N*′-nicotinoylquinoxaline-2-carbohydrazide, NRF2, KEAP1, Anti-inflammatory, Metabolic stability, Molecular docking

*Correspondence: tdevadoss@gmail.com; mallikarjunarao@imu.edu.my
†Murugesh Kandasamy and Kit-Kay Mak contributed equally to this work
[4] Center for Bioactive Molecules & Drug Delivery, Institute for Research, Development & Innovation, International Medical University, Kuala Lumpur, Malaysia
[5] KVSR Siddhartha College of Pharmaceutical Sciences, Vijayawada, Andhra Pradesh, India
Full list of author information is available at the end of the article

## Introduction

Lead generation is one of the key challenge in drug discovery and development process, and it is the search of chemical compounds that will be therapeutically effective against a disease. Fragment-based drug discovery (FBDD) is a technique often used to generate structures known as 'leads' [1]. From the literature search, a number of key structures were discovered to be potent anti-inflammatory agents. This includes quinoxaline [2], hydrazine [3] and pyridine. Thus, in this study, we aim to synthesised these fragments into a lead and to investigate its anti-inflammatory activity via Nrf2 activation.

Quinoxaline, fused ring of benzene and pyrazine, is one of the important class of heterocyclic compound having diverse biological activities [4–10] and present as integral part of diverse bioactive compounds and pharmaceuticals [11–15]. Hydrazines are nitrogen–nitrogen bond containing compounds which exhibit remarkable biological activities [16–19]. Pyridines possess many biological activities and present as an integral part of many medicinal compounds [20]. Quinoxalines substituted at second position are reported to possess remarkable biological activities [21]. Therefore, combining quinoxaline, hydrazine and pyridine moieties into one molecule as represented in Fig. 1 was believed to be a potential template for the synthesis of novel class of bioactive compounds.

Many reports in the literature demonstrated Nuclear factor erythroid 2 -related factor 2 (Nrf2) activation contributes to diverse biological activities by regulating the Kelch-like ECH-associated protein (Keap1)/Nrf2 signaling pathway [22–24]. Therefore Nrf2 activation has emerged as an attractive therapeutic approach to develop new classes of drugs as therapeutic treatment for a myriad of diseases and this includes inflammation, chronic multiple sclerosis, kidney disease, pulmonary fibrosis, cancer and chronic obstructive pulmonary disease (COPD) [25–32]. In literature, two well-studied Nrf2 activators were reported to be sulforaphane (a derived isothiocyanate from broccoli; and dimethyl fumarate, a new drug for the treatment of multiple sclerosis (Fig. 2). However, these two produce side effects due to the presence of strong electrophilic functional groups and hence covalently react with other proteins [33].

Another natural Nrf2 activator is oleanic triterpenoid bardoxolone imidazole. It was withdrawn from phase III clinical trials for patients diagnosed with type 2 diabetes and chronic kidney disease because of adverse cardiovascular events [34] that might be due to its covalent binding with key residues in protein. From these observations, it is postulated that the development of reversible covalent and non-covalent Nrf2 activators would be an ideal strategy to develop selective and safe Nrf2 activators [24, 35–38]. The above said efforts resulted in five series of compounds; tetrahydroisoquinoline, carbazone, naphthalene, thiopyrimidine and urea derivatives; that shown to activate Nrf2 whose representative structures were shown in Fig. 3.

It is noted that the proposed template and reported Nrf2 activators have few structural similarities. Therefore, in this study we synthesised the template compound, tested its efficacy in reversing the nitric oxide (NO) production, levels of pro-inflammatory cytokines (IL-1β, IL-6 and TNF-α), level of inflammatory mediator (Prostaglandin $E_2$ ($PGE_2$)) in LPS stimulated RAW 264.7 cells. Its' efficacy in disrupting the interaction between kelch domain of Keap 1 and Nrf2 was determined and in silico molecular docking studies were performed to acquire insights on its molecular interactions at the interface of Nrf2/Keap1. The metabolic stability profile of the compound was determined using liver microsomes (human, rat and mouse). We thought of proceeding with the synthesis of analogues only if the template compound showed promising anti-inflammatory and metabolic stability and therefore, the analogues were not synthesised.

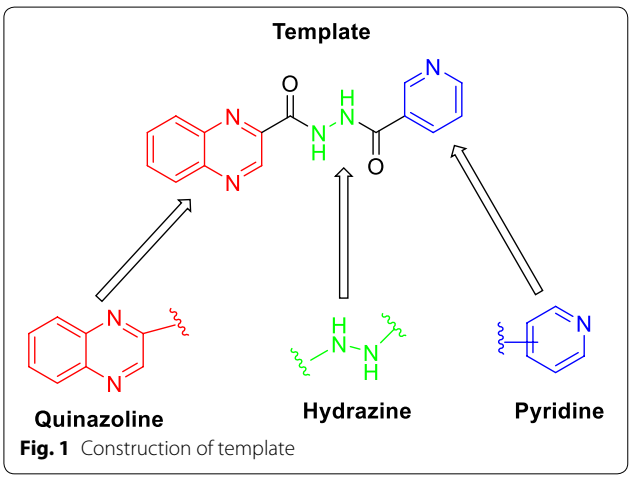


**Fig. 1** Construction of template

## Materials and methods

### General

*N*′-(Pyridine-3-carbonyl)quinoxaline-2-carbohydrazide (NQC) was synthesised and purified to 99.2% purity in International Medical University (IMU). Structure of the quinoxaline-2-carbohydrazide derivative was

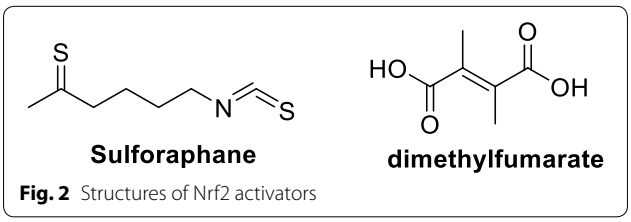


**Fig. 2** Structures of Nrf2 activators

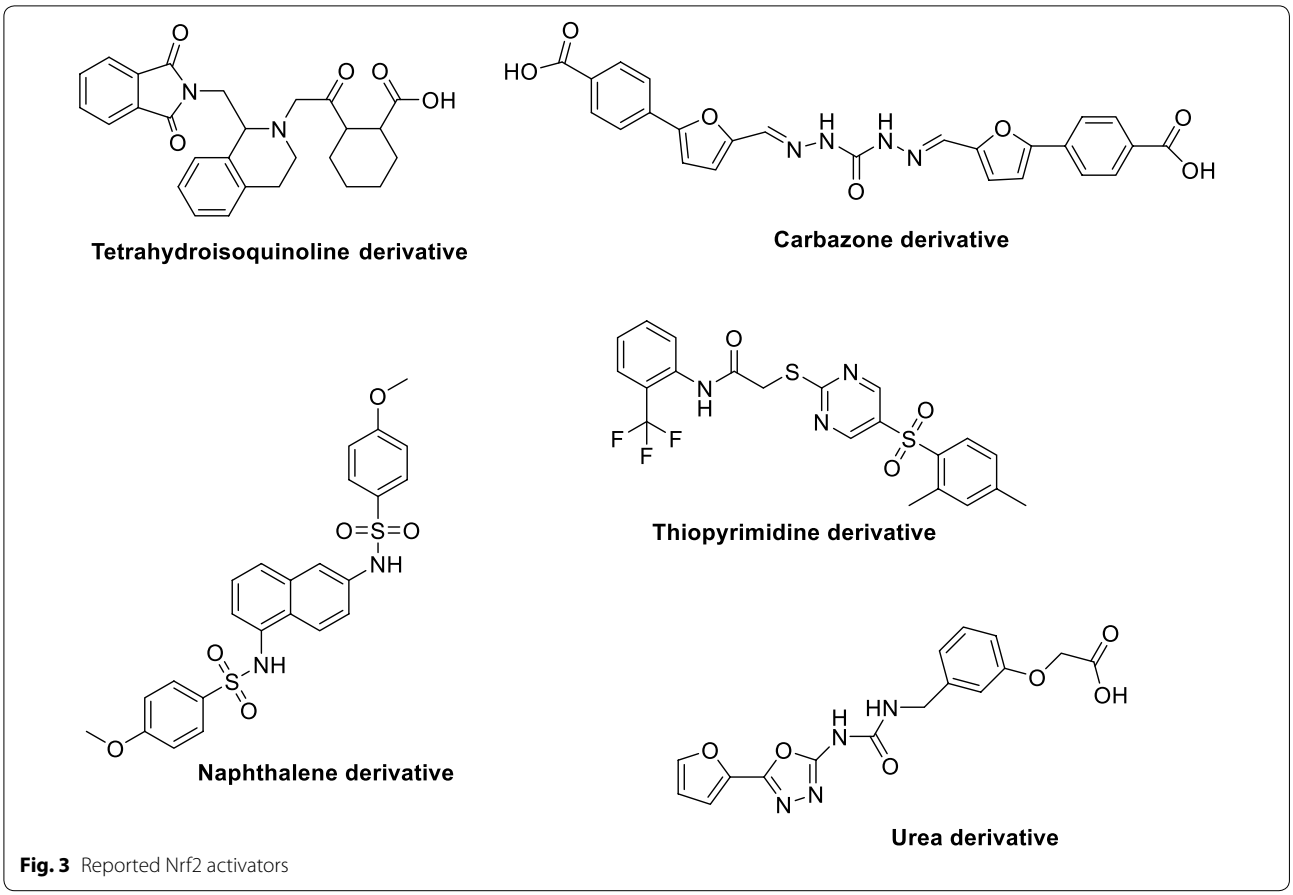


**Fig. 3** Reported Nrf2 activators

confirmed by spectroscopic methods. All solvents used in this research were of high performance column chromatography (HPLC) grade. Chemical reagents including formic acid and dipotassium phosphate ($K_2HPO_4$) from Fisher Scientific, dimethyl sulfoxide (DMSO) and monopotassium phosphate ($KH_2PO_4$) from Merck, and acetonitrile (ACN) from Friedemann Schmidt were used. (3-(4,5-Dimethylthiazol-2-yl)-2,5-Diphenyltetrazolium Bromide), sulphanilamide, *N*-(1-naphthyl)ethylenediamine and biological grade DMSO were procured from Sigma-Aldrich Sdn. Bhd, Malaysia. β-NADPH was procured from Sigma Aldrich, USA. RAW 264.7 cells and LPS (*Escherichia coli* O111:b4) were procured from American Type Culture Collection, Manassas, USA. HLM, RLM and MLM (20 mg/mL, Catalog #HMMCPL, Gibco) was procured from Life Technologies, Singapore.

Synthesis of *N*′-(pyridine-3-carbonyl)quinoxaline-2-carbohydrazide is as shown in Fig. 4.

### Cell culture

Murine macrophages, cell line: RAW 264.7 was procured from ATCC, USA. The macrophage cells were grown and cultured in Dulbecco's Modified Eagle Medium (DMEM) supplemented with 10% Fetal Bovine serum (FBS) and 1% PenStrep and incubated in a 5% $CO_2$ at 37 °C incubator. Cells from passages 10 to 20 were used for subsequent experiments.

### Cell viability

A calorimetric agent (3-(4,5-Dimethylthiazol-2-yl)-2,5-Diphenyltetrazolium Bromide) (MTT) was used to as an assay to determine cell viability after being exposed to NQC. RAW 264.7 cells were seeded in a 96-well microplate at $3 \times 10^5$ cells/well and were allowed to grow and adhere for 24 h in a 37 °C, 5% $CO_2$ incubator. NQC was dissolved in DMSO and diluted with PBS to produce the required test concentrations (100, 50, 25, 12.5, 6.25 and 3.125 μM). The negative control is 0.1% (v/v) DMSO, which is the maximum effective concentration of DMSO in a well. The cells were treated with either NQC or 0.1% (v/v) DMSO for 4 h followed by 1 μg/mL LPS*Ec* and incubated further for 20 h. MTT solution was added at 100 μL per well under dark condition and the cells were incubated further for 4 h. Upon completion of incubation, the contents in all wells were aspirated and DMSO was added at 100 μL per well. The absorbance was measured

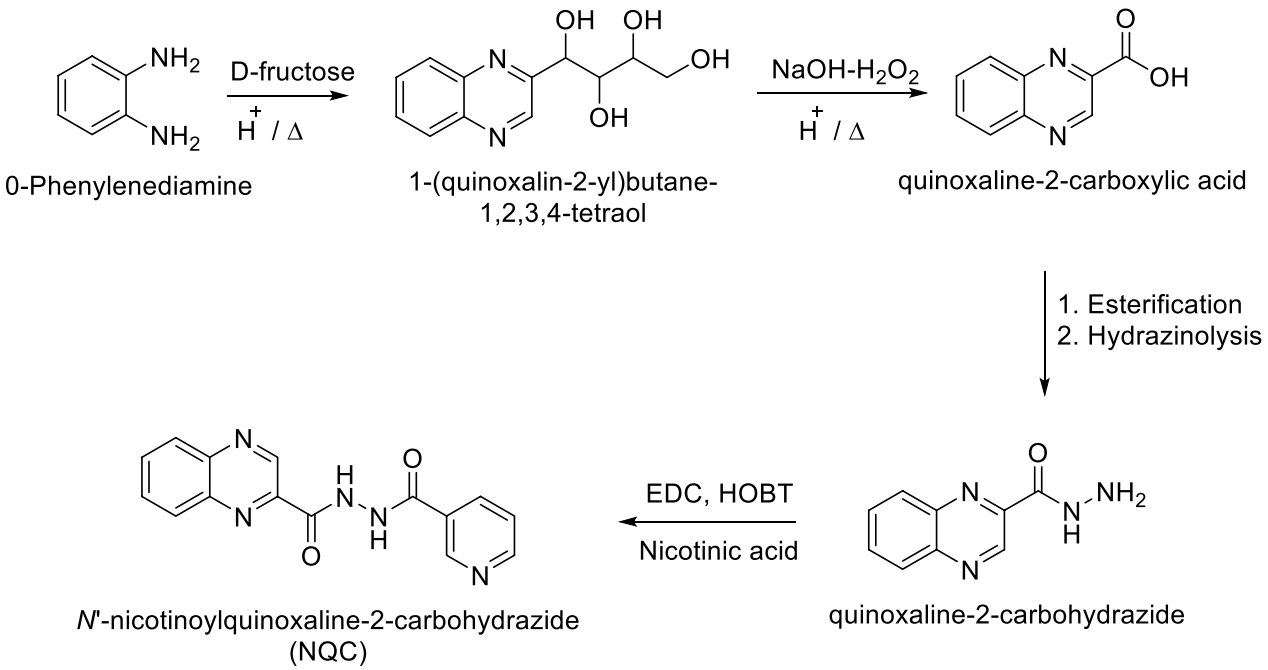


**Fig. 4** Synthetic route of *N*′-(pyridine-3-carbonyl) quinoxaline-2-carbohydrazide (NQC)

at 570 nm using Molecular Devices Spectramax M3 Multi-Mode microplate reader; Sunnyvale, CA, USA. The cells without any treatment was used as a control. MTT assay was performed in triplicate. The percent cell viability is calculated using the following equation:

$$Percent\ Cell\ Viabilty = \frac{Absorbance\ of\ Vehicle\ or\ TD\ -\ 1\ treated\ group\ well}{Absorbance\ of\ Control\ well} \times 100.$$

#### Determination of nitric oxide (NO)

RAW 264.7 cells were seeded in a 96-well microplate at $3 \times 10^5$ cells/well with complete media. The cells were allowed grow and adhere for 24 h. The cells were treated with NQC (50, 25, 12.5, 6.25 and 3.125 µM) and negative control (0.1% v/v DMSO in water) for 4 h prior to LPS*Ec* (1 µg/mL) and allowed to incubate for 20 h at 37 °C, 5% $CO_2$ incubator. Nitrite exist as a stable metabolite of nitric oxide, thus nitrite present in the supernatant was quantitatively measured as a chemical marker of nitric oxide (NO) production using Griess reagent (Promega, USA; 0.1% naphthylethylenediamine dihydrochloride and 1% sulfanilamide in 2.5% phosphoric acid). This assay was carried out following the manufacturer's protocol where 100 µL of cell supernatant sample was incubated with 100 µL of Griess reagent at room temperature for 10 min and the absorbance at 540 nm was measured using Molecular Devices Spectramax M3 Multi-Mode microplate reader. A standard curve of sodium nitrite was plotted and used as a reference for extrapolation to quantify the amount of nitrite present.

#### Determination of IL-1β, IL-6, $PGE_2$, and TNF-α

Production of IL-1β, IL-6, $PGE_2$, and TNF-α in RAW 264.7 cells were quantitatively measured using an enzyme-linked immunosorbent assay (ELISA). The cells were incubated with 0.1% DMSO or NQC for 4 h, then stimulated with LPS*Ec*, 1 µg/mL, for 20 h. The production of pro-inflammatory cytokines (IL-1β, IL-6) and TNF-α were determined using commercial ELISA kit (RayBio) according to the manufacturer's instructions in product insert. The absorbance was measured at 540 nm. All the experiments were performed in triplicate.

#### Nrf2 activation assay

The Nrf2 activation by NQC was determined using 'Keap1:Nrf2 Inhibitor Screening Assay Kit' (BPS Bioscience, USA) following the instructions in product insert. The NQC was dissolved in DMSO and diluted with assay buffer provided in the kit to produce the concentrations

range, 100 μM to 1 nM. The fluorescence of the solutions in each well of 96-well plate was measured at $\lambda_{ex}$ 485 nm and $\lambda_{em}$ 530 nm. The dose–response curve was constructed plotting percent reduction in Kepa1-Nrf2 binding activity versus log concentration of NQC. From dose–response curve $IC_{50}$ value was calculated.

### Molecular docking studies

To acquire molecular insights on the binding mode of NQC in Keap-1 binding site, molecular docking studies were carried out. Schrödinger small-molecule drug discovery suite 2018-2 was used to perform in silico docking studies. The crystal structure (PDB code: 5CGJ) used was sourced from 'Research Collaboratory for Structural Bioinformatics Protein Data Bank' (PDB) (http://www.pdb.org). The 'protein preparation wizard' was used to prepare the protein for molecular docking studies. This was followed by grid generation using 'receptor grid generation wizard' with default settings. The chemical structure of NQC was sketched in Maestro and prepared for docking using 'ligprep' wizard. Docking between the low energy conformation of NQC onto the binding site was performed by selecting the extra precision (XP) mode where protein–ligand structural motifs and water desolvation energy are incorporated to account for scoring function of binding free energy. The binding poses and affinity was further confirmed where "Induced Fit Docking' (IFD) module was applied to NQC into the binding site. IFD module is docking protocol "Glide" and "Prime" where ligand flexibility and receptor flexibility are accounted for. GlideSP feature generates softened-potential docking protocol and was used to generate an initial number of 20 poses in the primary stage of IFD. Residues of the protein below 5.0 Å of ligand for each pose were refined. Docking of ligands from this is run again using GlideSP to generate poses. The top-ranked dock poses' binding free energy (ΔG°) were calculated using the module Prime/Molecular Mechanics-Generalized Born Surface Area (MM-GBSA) with default settings.

### Metabolic stability assessment of NQC

A stock solution (SS) of NQC at 1 mM was prepared using 100% dimethyl sulfoxide. Working solution of 10 μM was further prepared by dilution of SS with 25% ACN and 50 mM tris–HCl buffer (pH 7.4). In a 96-well plate, NQC (effective concentration:1 μM) was incubated with phosphate buffer (pH7.4) and 0.5 mg/mL of liver microsomes (human, rat and mouse) at 37 °C in an incubation. Each NQC incubation with liver microsomes was performed in triplicates. The microsomal metabolic reaction was initiated by the addition of co-factor, NADPH (5 mM). Samples following the allotted time-point was drawn and quenched into a solution of acetonitrile containing 50 ng/mL internal standard. The sample was analysed by a developed HPLC method that has been validated for lower limit of quantification, linearity, precision, selectivity and accuracy according to FDA guidance [39].

Half-life of NQC was calculated using the equation:

$$T_{1/2} = \frac{0.693}{K}.$$

The in vitro microsomal intrinsic clearance ($CL_{int}$) was calculated based on the equation below:

$$Cl_{int} = \left[\frac{0.693}{in\ vitro\ t_{(1/2)}}\right] \times \left[\frac{\text{ml } incubation}{\text{mg } microsome}\right] \times \left[\frac{52.5 \text{ mg } microsome}{\text{g } liver}\right] \times \left[\frac{52.5 \text{ mg } liver}{\text{kg } bw}\right].$$

### Statistical analysis

The results were analysed and data are reported as mean ± standard deviation. The significance of the values was determined using student *t* test. Statistical significant difference was defined as P-value less than 0.05 ($P < 0.05$). All the statistical analyses were performed using Micosoft Excel.

## Results and discussion

### Characterisation of NQC

NQC was successfully synthesised and the chemical compound was spectroscopically elucidated using $^{1}H$ Nuclear Magnetic Resonance (NMR), $^{13}C$ Nuclear Magnetic Resonance, Fourier transform-infrared spectroscopy (FT-IR), and mass spectroscopy (MS). The overall schematic representation is as shown in Fig. 3. The target compound was synthesised and tested for purity by thin layer chromatography (TLC) using hexane and ethyl acetate (1:1) as the solvent system, and the $R_f$ value calculated was 0.32. Structure of the compound was elucidated and confirmed using $^{1}H$ NMR, $^{13}C$ NMR, FT-IR and MS.

Pale brown solid; Yield 80%; mp 203 °C; FT-IR; $\nu$/$cm^{-1}$ = 3311.78 (NH), 1643.35 (CO), 1579.70 (NH), 1535.34 (C=C); $^{1}H$ NMR (600 MHz, DMSO-$d_6$,): $\delta_{ppm}$ = 11.00 (s, 2H), 9.48 (d, 1H), 9.08 (1, $J$ = 2.4 Hz, 1H), 8.74–8.73 (d, $J$ = 6.0 Hz, 1H), 8.27–8.22 (q, 12.0, 6.0 Hz, 2H), 8.22–8.20 (q, $J$ = 6.0 Hz, 2H), 7.55–7.53 (m, $J$ = 6.0 Hz, 1H); $^{13}C$ NMR (150 MHz, DMSO-$d_6$): $\delta_{ppm}$ = 164.8, 161.4, 148.7, 148.1, 144.0, 143.8, 142.9, 140.3, 135.3, 131.9, 130.7, 130.3, 128.9, 125.1; MS (m/z) (%) = 293 (100), 294 (16.2), 295 (0.9), 296 (0.9). Analysis for $C_{15}H_{11}N_5O_2$ (293.29): calcd.: C, 61.43; H, 3.78; N, 23.88; O, 10.91%; found: C, 61.55; H, 3.75; N, 23.79; O, 10.95%.

### Cell viability

The main purpose of this assay is to determine the NQC concentration range which is non-toxic to RAW 264.7 cells. The cytotoxicity effects of NQC (at a range of concentration) against RAW 264.7 cells stimulated with LPS*Ec* was performed using calorimetric MTT assay. Based on the results depicted in Fig. 5a, NQC do not show cytotoxic effects on RAW 264.7 cells at the tested concentrations of 3.125–50 μM ($P > 0.05$), while NQC at 100 μM shows significant toxicity ($P < 0.05$). Therefore, based on these results, NQC with concentrations between 3.125 and 50 μM was used for the subsequent experiments.

### Effect of NQC on NO production

NO production as an inflammatory mediator in the cell culture medium of LPS*Ec* stimulated RAW 264.7 cells is deduced using the Griess reaction [40]. The results are shown in Fig. 5b. The concentration of NO increased significantly in the LPS*Ec* stimulated RAW 264.7 cells (LPS*Ec* + DMSO) ($P < 0.05$) when compared to normal control (no LPS*Ec* + DMSO). This shows that NO production was induced by LPS*Ec* in RAW 264.7 cells. NQC between 3.125 and 50 μM significantly reversed the production of NO in LPS*Ec* induced RAW 264.7 cells in a dose-dependent manner ($P < 0.05$). It was reported that NO is involved in the regulation of multistage processes found in inflammation—particularly in the initial stages of inflammatory cells transmigrating to inflammation sites [41]. Therefore, NQC is found to be potent anti-inflammatory agent with an $IC_{50}$ value of $26.13 \pm 1.17$ μM.

### Effect of NQC on pro-inflammatory cytokines (IL-1β, IL-6 and TNF-α) and $PGE_2$

Inflammatory mediators and cytokines highly mediates inflammatory response especially in the initial stages of inflammation. These includes $PGE_2$, NO; and pro-inflammatory cytokines namely IL-1β, IL-6 and TNF-α [42]. Subsequently, these cytokines will be responsible as upstream mediators where other inflammatory cytokines will be further stimulated and emitted, and ultimately leads to critical clinical symptoms of pain and its related immune disorders [43]. Therefore, the effects of NQC on inhibiting the production of IL-1β, IL-6, $PGE_{2-}$ and TNF-α in the LPS*Ec* stimulated RAW 264.7 cells were quantitatively measured using ELISA. As depicted in Fig. 5c–f, the results from ELISA showed that the NQC in LPS*Ec* stimulated RAW 264.7 cells mediated the production of inflammatory cytokines and mediators at a dose-dependent manner compared to the negative control ($P < 0.05$) with $IC_{50}$ values $13.27 \pm 2.37$, $10.13 \pm 0.58$, $14.41 \pm 1.83$ and $15.23 \pm 0.91$ μM respectively.

In the current study, it was found that NQC dramatically reduced the high levels of inflammatory mediators, NO radicals and $PGE_2$, and pro-inflammatory cytokines of IL-1β, IL-6 and TNF-α stimulated by LPS*Ec* (Fig. 1b–f). In conclusion, it is believed that the NQC exerts desirable anti-inflammatory activity via suppression of excessive inflammatory mediators and inflammatory factors produced during inflammation.

### Effect of NQC on Nrf2 activation

Nrf2 is a transcription factor protein that contributes to the anti-inflammatory process by playing the role as an upstream regulator through binding with antioxidant response element (ARE); and is responsible in recruiting inflammatory cells and regulating gene expression. Anti-inflammatory gene expression and inhibition of inflammatory progression is regulated by Keap1/Nrf2/ARE signaling pathway. Under normal homeostasis conditions, Nrf2 remains ubiquitously bounded to the cytoskeletal protein Keap1. Due to Nrf2 activation, an anti-inflammatory response ensues. Thus, we determined the activity of NQC in inhibiting Nrf2-Keap1 interaction. The NQC showed dose-dependent activity in inhibiting Nrf2-Keap1interaction as shown in Fig. 2 and its $IC_{50}$ value was $4.21 \pm 0.89$ μM.

### Molecular docking studies

The primary docking of NQC with the binding pocket of 5CGJ was performed using Glide XP protocol where the flexibility of both ligand and receptor were disregarded. Here, favorable binding score of NQC at −4.806 kcal/mol and ligand efficiency of −0.218 kcal/mol were observed. Induced Fit Docking protocol was performed for NQC into the binding pocket where the introduction of residue flexibility is below 5 Å from the ligand. The IFD protocol presented highly negative IFD score (−647.102 kcal/mol) indicating it is a favorable binding energy; and highly negative XP G score (−7.051 kcal/mol). The binding free energy of the NQC was computed using MM-GBSA approach to further confirm it's binding. The binding free energies of NQC was −47.801 kcal/mol. The collective results give a confidence that NQC binds strongly in the binding site of Nrf2/Keap1 interface, which could be responsible for inhibition of Nrf2/Keap1 interaction. The 3D- and 2D-interaction diagram of NQC in the binding site of Nrf2/Keap1 interface is shown in Fig. 6b, c. As shown in the figures, the NQC forms hydrogen bond interactions with Ser 602 and Arg 415; hydrophobic interactions with Tyr 334, Ala 510, Ala 556, Ala 557, Ala 559, Phe 577 and Val 604.

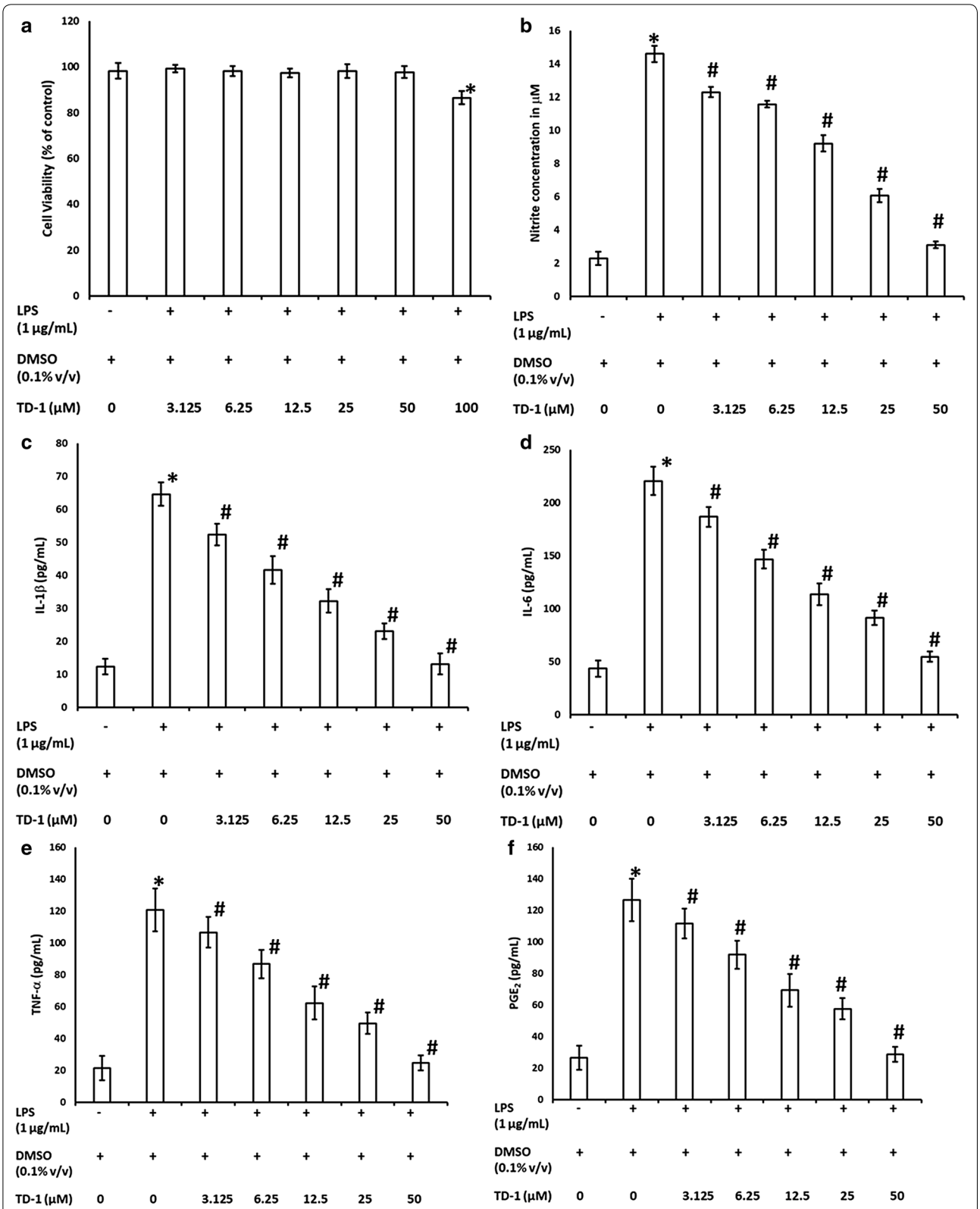


**Fig. 5** In vitro anti-inflammatory activity of TD-1 on RAW 264.7 cells. The effect of TD-1 on **a** cell viability; **b** LPS stimulated nitrite production; **c** LPS stimulated IL-1β production; **d** LPS stimulated 1L-6 production; **e** LPS stimulated TNF-α production and **f** LPS stimulated $PGE_2$ production. In **a**; *Significant difference ($P < 0.05$) with respect to the cells (DMSO + LPS) treatment. In **b**–**f**; *Significant difference with respect to the cells (only DMSO treatment), #Significant difference with respect to the cells (LPS + DMSO) treatment

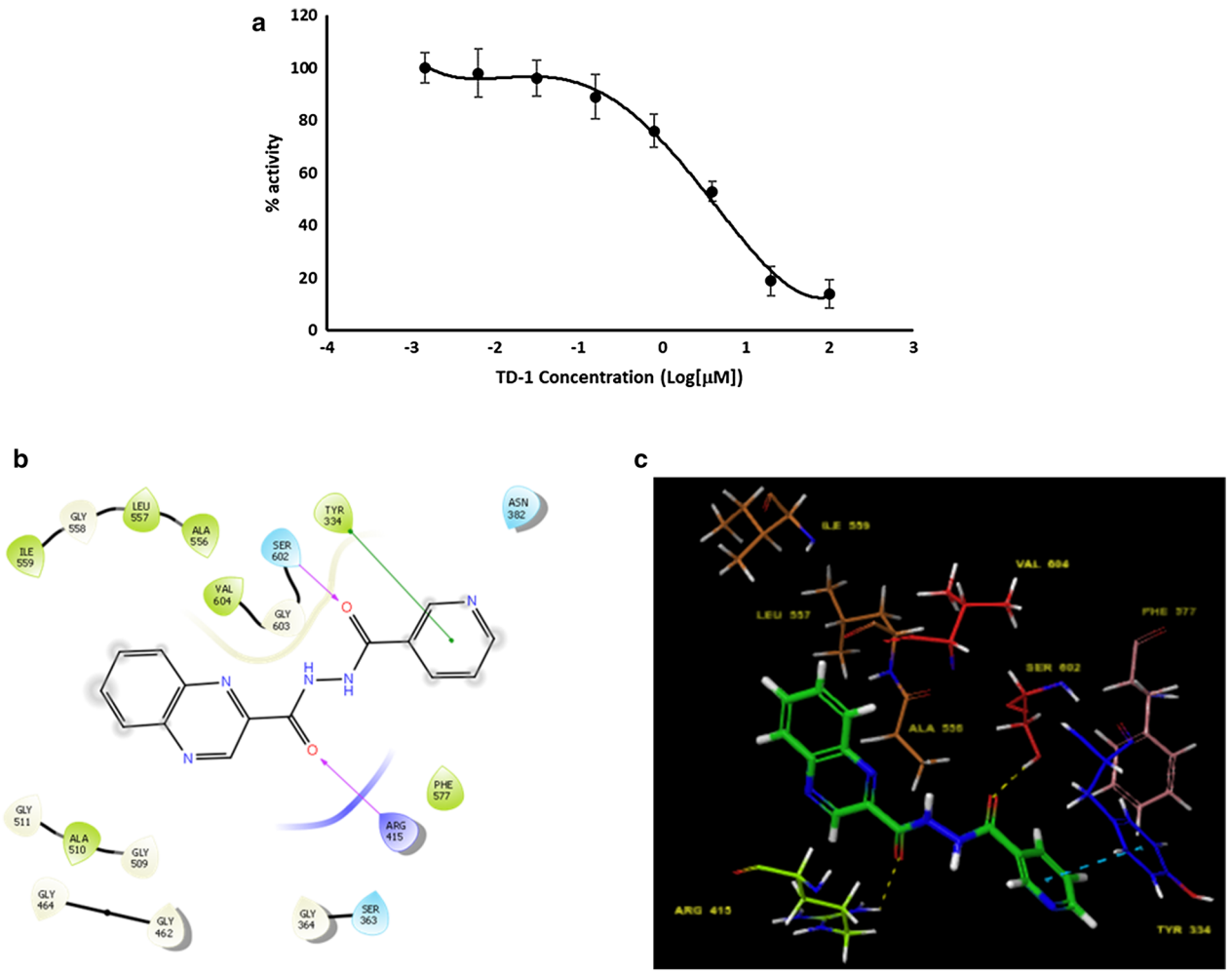


**Fig. 6** Nrf2 activation of TD-1. **a** The dose–response effect of TD-1 on inhibition of Nrf2/Keap1 interaction. **b** The 2D-intreraction diagram depicting H-bond, hydrophobic and pi-pi interactions between TD-1 and amino acid residues of the binding pocket of Nrf2/Keap1 interface (PDB ID: 5CGJ). The residues with light green shade denote the amino acids that form hydrophobic interactions with TD-1. **c** The 3D-interaction diagram showing interaction between TD-1 and key amino acid residues of binding pocket of 5CGJ

**Table 1 The microsomal intrinsic clearance of NQC of different species' liver microsomes calculated based on the available data**

| Species of liver microsome | $T_{1/2}$ (min) | $mC_{int}$ (mL/min/g liver) | Rate of metabolism ($min^{-1}$) |
|---|---|---|---|
| Human | 63.30 ± 1.73 | 1.14 ± 0.31 | 0.011 |
| Rat | 52.23 ± 0.81 | 1.39 ± 0.87 | 0.013 |
| Mouse | 24.55 ± 1.13 | 2.96 ± 0.34 | 0.028 |

### Metabolic stability studies

A calibration curve of peak area against the nominal concentrations of NQC was prepared using linear least-square regression model. The lower limit of quantitation (LLOQ) was determined to be 0.01 μM. The signal:noise ratio was found to be greater than 10. The linearity of the assay was r > 0.995 when assessed on the concentration range of 0.01–2.00 μM which is above the desired level of > 0.990. The assessment on intra- and inter-day precision and accuracy were carried out on three successive days using three concentration (0.02, 0.5 and 1.6 μM) where the intra- and inter-day precisions (RSD %) was less than 9.00% and the accuracy (RE %) fell in the range of − 2.12 to 5.23%. The determination of NQC extraction recovery at three concentrations, 0.02, 0.5 and 1.6 μM was carried out and was achieved by comparing the peak area of extracted analyte in six replications (n = 6) with blank samples of post-extraction. The mean recovery was observed to be > 85.95%.

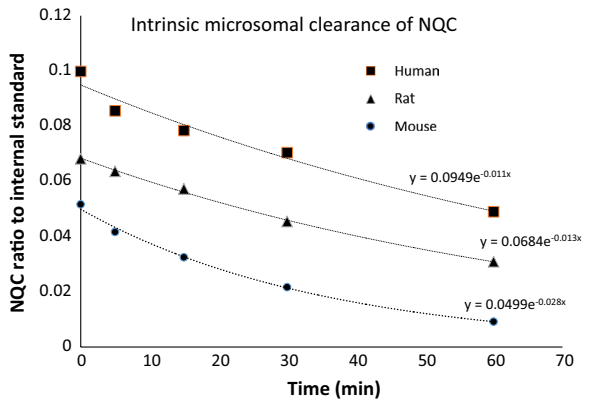


**Fig. 7** Intrinsic microsomal clearance of NQC in human, rat and mouse liver microsomes over time

In vitro microsomal metabolic stability assay using human, rat and mouse liver microsomes were performed to estimate half-life and microsomal intrinsic clearance of NQC at an effective concentration of 1 µM. The ratio of NQC to internal standard over time for human, rat and mouse liver microsomes are shown in Fig. 7 and the coefficient of correlations were more than 0.97. The observe in vitro $T_{1/2}$ ($63.30 \pm 1.73$, $52.33 \pm 0.81$ and $24.55 \pm 0.34$ min in human, rat and mouse respectively) as shown in Table 1, indicated that NQC presented faster clearance in mouse liver microsomes upon stimulation by the co-factor, NADPH. Whereas NQC presented moderate microsomal metabolism in rat and human liver microsomes. Correspondingly, the observed in vitro $CL_{int}$ ($1.14 \pm 0.31$, $1.39 \pm 0.87$ and $2.96 \pm 0.34$ µL/min/g liver in human, rat and mouse respectively) revealed that NQC displayed moderate stability (< 5 mL/min/g liver) in human, rat and mouse. From this in vitro assay, rat seems to have a closer value to human than that of mouse. From these findings, rat would be a suitable animal model for in vivo pharmacokinetics and metabolism of NQC in human.

#### Abbreviations

NRF2: nuclear factor erythroid-2-related factor 2; KEAP1: Kelch-like ECH-associated protein; NQC: *N*′-nicotinoylquinoxaline-2-carbohydrazide; LPSEc: lipopolysaccharide from *Escherichia coli*; IL: interleukin; TNF-α: tumor necrosis factor-α; $PGE_2$: prostaglandin $E_2$; $IC_{50}$: inhibitory concentration, 50%; FBDD: fragment-based drug discovery; NO: nitric oxide; DMSO: dimethylsulfoxide; NADPH: reduced form of nicotinamde adenine dinucleotide phosphate; HLM: human liver microsomes; RLM: rat liver microsomes; MLM: mouse liver microsomes; DMEM: Dublecco's modified eagle medium; FBS: fetal bovine serum; MTT: 3-(4,5-dimethylthiazol-2-yl)-2,5-diphenylterazolium bormide; PBS: phosphate buffer saline; ELISA: enzyme-linked immnosorbent assay; PDB: protein data bank; IFD: induced fit docking; SP: standard precision; MM-GBSA: molecular mechanics-generalized born surface area; HPLC: high performance liquid chromatography; FDA: food and drug administration; TLC: thin layer chromatography; NMR: nuclear magnetic resonance; MS: mass spectroscopy; FT-IR: Fourier transform infrared.

#### Acknowledgements

The authors would like to thank International Medical University for providing the facilities.

#### Authors' contributions

Authors MRP and TD designed the research. MK, HC and K-KM done metabolic stability studies. TD and RS synthesised the compound. PVT and K-KM did the anti-inflammatory studies. K-KM did the molecular docking studies. All authors contributed equally in writing the paper. All authors read and approved the final manuscript.

#### Funding

This work was funded by Ministry of Higher Education, Malaysia through Fundamental Research Grant Scheme (FRGS); FRGS/1/2014/SG01/IMU/03/1.

#### Availability of data and materials

All data generated or analysed during this study are included in this published article.

#### Competing interests

The authors declare that they have no competing interests.

#### Author details

[1] Department of Pharmaceutical Chemistry, School of Pharmacy, International Medical University, Kuala Lumpur, Malaysia. [2] School of Postgraduate Studies and Research, International Medical University, Kuala Lumpur, Malaysia. [3] Department of Pharmaceutical Technology, School of Pharmacy, International Medical University, Kuala Lumpur, Malaysia. [4] Center for Bioactive Molecules & Drug Delivery, Institute for Research, Development & Innovation, International Medical University, Kuala Lumpur, Malaysia. [5] KVSR Siddhartha College of Pharmaceutical Sciences, Vijayawada, Andhra Pradesh, India. [6] ISF College of Pharmacy, Moga, Punjab, India. [7] Department of Chemistry, Central University of Karnataka, Gulbarga, Kanataka, India.

Received: 9 July 2019 Accepted: 10 September 2019
Published online: 24 September 2019

#### References

1. Lanter J, Zhang X, Sui Z (2011) Medicinal chemistry inspired fragment-based drug discovery. In: Methods enzymology, pp 421–45. https://doi.org/10.1016/b978-0-12-381274-2.00016-9
2. Tariq S, Somakala K, Amir M (2018) Quinoxaline: an insight into the recent pharmacological advances. Eur J Med Chem 143:542–557. https://doi.org/10.1016/J.EJMECH.2017.11.064
3. Tafazoli S, Mashregi M, O'Brien PJ (2008) Role of hydrazine in isoniazid-induced hepatotoxicity in a hepatocyte inflammation model. Toxicol Appl Pharmacol 229:94–101. https://doi.org/10.1016/j.taap.2008.01.002
4. Burguete A, Pontiki E, Hadjipavlou-Litina D, Ancizu S, Villar R, Solano B, Moreno E, Torres E, Pérez S, Aldana I, Monge A (2011) Synthesis and biological evaluation of new quinoxaline derivatives as antioxidant and anti-inflammatory agents. Chem Biol Drug Des 77:255–267. https://doi.org/10.1111/j.1747-0285.2011.01076.x
5. Nakhi A, Rahman MS, Kishore R, Meda CLT, Deora GS, Parsa KVL, Pal M (2012) Pyrrolo[2,3-b]quinoxalines as inhibitors of firefly luciferase: their Cu-mediated synthesis and evaluation as false positives in a reporter gene assay. Bioorganic Med Chem Lett 22:6433–6441. https://doi.org/10.1016/j.bmcl.2012.08.056
6. Wu K, Ai J, Liu Q, Chen T, Zhao A, Peng X, Wang Y, Ji Y, Yao Q, Xu Y, Geng M, Zhang A (2012) Multisubstituted quinoxalines and pyrido[2,3-d] pyrimidines: synthesis and SAR study as tyrosine kinase c-Met inhibitors. Bioorganic Med Chem Lett 22:6368–6372. https://doi.org/10.1016/j.bmcl.2012.08.075
7. Patidar AK, Jeyakandan M, Mobiya AK, Selvam G (2011) Exploring potential of quinoxaline moiety. Int J PharmTech Res 3:386–392
8. Pereira JA, Pessoa AM, Cordeiro MNDS, Fernandes R, Prudêncio C, Noronha JP, Vieira M (2015) Quinoxaline, its derivatives and applications: a State of the Art review. Eur J Med Chem 97:664–672. https://doi.org/10.1016/j.ejmech.2014.06.058

9. RaghavendraRao K, Raghunadh A, Kalita D, Laxminarayana E, Pal M, Meruva SB (2015) Biological activity of drug like small molecules based on quinoxaline containing amino substitution at C-2. Der Pharma Chem. 7:77–85
10. Moody CJ, Swann E, Houlbrook S, Stephens MA, Stratford IJ (2015) synthesis and biological activity of quinoxaline derivatives. World J Pharm Res 4:1892–1900. https://doi.org/10.1007/s11094-014-1128-1
11. Burguete A, Pontiki E, Hadjipavlou-Litina D, Villar R, Vicente E, Solano B, Ancizu S, Pérez-Silanes S, Aldana I, Monge A (2007) Synthesis and anti-inflammatory/antioxidant activities of some new ring substituted 3-phenyl-1-(1,4-di-N-oxide quinoxalin-2-yl)-2-propen-1-one derivatives and of their 4,5-dihydro-(1H)-pyrazole analogues. Bioorg Med Chem Lett 17:6439–6443. https://doi.org/10.1016/j.bmcl.2007.10.002
12. Smits RA, Lim HD, Hanzer A, Zuiderveld OP, Guaita E, Adami M, Coruzzi G, Leurs R, de Esch IJP (2008) Fragment based design of new $H_4$ receptor — ligands with anti-inflammatory properties in vivo. J Med Chem 51:2457–2467. https://doi.org/10.1021/jm7014217
13. Jaso A, Zarranz B, Aldana I, Monge A (2005) Synthesis of new quinoxaline-2-carboxylate 1,4-dioxide derivatives as anti-Mycobacterium tuberculosis agents. J Med Chem 48:2019–2025. https://doi.org/10.1021/jm049952w
14. Rong F, Chow S, Yan S, Larson G, Hong Z, Wu J (2007) Structure–activity relationship (SAR) studies of quinoxalines as novel HCV NS5B RNA-dependent RNA polymerase inhibitors. Bioorg Med Chem Lett 17:1663–1666. https://doi.org/10.1016/j.bmcl.2006.12.103
15. Hazeldine ST, Polin L, Kushner J, White K, Bouregeois NM, Crantz B, Palomino E, Corbett TH, Horwitz JP (2002) Synthesis and biological evaluation of some bioisosteres and congeners of the antitumor agent, 2-(4-[(7-chloro-2-quinoxalinyl)oxy]phenoxy)propionic acid (XK469). J Med Chem 35:3130–3137. https://doi.org/10.1021/jm0200097
16. Kajal A, Bala S, Sharma N, Kamboj S, Saini V (2014) Therapeutic potential of hydrazones as anti-inflammatory agents. Int J Med Chem 2014:761030. https://doi.org/10.1155/2014/761030
17. Le Goff G, Ouazzani J (2014) Natural hydrazine-containing compounds: biosynthesis, isolation, biological activities and synthesis. Bioorganic Med Chem 22:6529–6544. https://doi.org/10.1016/j.bmc.2014.10.011
18. Narang R, Narasimhan B, Sharma S (2012) A review on biological activities and chemical synthesis of hydrazide derivatives. Curr Med Chem 19:569–612. https://doi.org/10.2174/092986712798918789
19. Rollas S, Küçükgüzel ŞG (2007) Biological activities of hydrazone derivatives. Molecules 12:1910–1939. https://doi.org/10.3390/12081910
20. Altaf AA, Shahzad A, Gul Z, Rasool N, Badshah A, Lal B, Khan E (2015) A review on the medicinal importance of pyridine derivatives. Sci Publish Group. 1:1. https://doi.org/10.11648/J.JDDMC.20150101.11
21. Kumar KS, Rambabu D, Sandra S, Kapavarapu R, Krishna GR, Basaveswara-Rao MV, Chatti K, Reddy CM, Misra P, Pal M (2012) AlCl3induced (hetero) arylation of 2,3-dichloroquinoxaline: a one-pot synthesis of mono/disubstituted quinoxalines as potential antitubercular agents. Bioorganic Med Chem 20:1711–1722. https://doi.org/10.1016/j.bmc.2012.01.012
22. Winkel AF, Engel CK, Margerie D, Kannt A, Szillat H, Glombik H, Kallus C, Ruf S, Güssregen S, Riedel J, Herling AW, Von Knethen A, Weigert A, Brüne B, Schmoll D (2015) Characterization of RA839, a noncovalent small molecule binder to Keap1 and selective activator of Nrf2 signaling. J Biol Chem 290:28446–28455. https://doi.org/10.1074/jbc.M115.678136
23. Jain AD, Potteti H, Richardson BG, Kingsley L, Luciano JP, Ryuzoji AF, Lee H, Krunic A, Mesecar AD, Reddy SP, Moore TW (2015) Probing the structural requirements of non-electrophilic naphthalene-based Nrf2 activators. Eur J Med Chem 103:252–268. https://doi.org/10.1016/j.ejmech.2015.08.049
24. Marcotte D, Zeng W, Hus JC, McKenzie A, Hession C, Jin P, Bergeron C, Lugovskoy A, Enyedy I, Cuervo H, Wang D, Atmanene C, Roecklin D, Vecchi M, Vivat V, Kraemer J, Winkler D, Hong V, Chao J, Lukashev M, Silvian L (2013) Small molecules inhibit the interaction of Nrf2 and the Keap1 Kelch domain through a non-covalent mechanism. Bioorganic Med Chem 21:4011–4019. https://doi.org/10.1016/j.bmc.2013.04.019
25. Lee JS, Surh YJ (2005) Nrf2 as a novel molecular target for chemoprevention. Cancer Lett 224:171–184. https://doi.org/10.1016/j.canlet.2004.09.042
26. Zhao CR, Gao ZH, Qu XJ (2010) Nrf2-ARE signaling pathway and natural products for cancer chemoprevention. Cancer Epidemiol 34:523–533. https://doi.org/10.1016/j.canep.2010.06.012
27. Kwak MK, Kensler TW (2010) Targeting NRF2 signaling for cancer chemoprevention. Toxicol Appl Pharmacol 244:66–76. https://doi.org/10.1016/j.taap.2009.08.028
28. Yang L, Palliyaguru DL, Kensler TW (2016) Frugal chemoprevention: targeting Nrf2 with foods rich in sulforaphane. Semin Oncol 43:146–153. https://doi.org/10.1053/j.seminoncol.2015.09.013
29. Keum Y-S, Jeong W-S, Kong ANT (2004) Chemoprevention by isothiocyanates and their underlying molecular signaling mechanisms. Mutat Res 555:191–202. https://doi.org/10.1016/j.mrfmmm.2004.05.024
30. Kikuchi N, Ishii Y, Morishima Y, Yageta Y, Haraguchi N, Itoh K, Yamamoto M, Hizawa N (2010) Nrf2 protects against pulmonary fibrosis by regulating the lung oxidant level and Th1/Th2 balance. Respir Res. https://doi.org/10.1186/1465-9921-11-31
31. Gold R, Kappos L, Arnold DL, Bar-Or A, Giovannoni G, Selmaj K, Tornatore C, Sweetser MT, Yang M, Sheikh SI, Dawson KT (2012) Placebo-controlled phase 3 study of oral BG-12 for relapsing multiple sclerosis. N Engl J Med 12367:1098–1107. https://doi.org/10.1056/NEJMoa1114287
32. Crunkhorn S (2012) Deal watch: abbott boosts investment in NRF2 activators for reducing oxidative stress. Nat Rev Drug Discov 2012:112
33. Hu C, Eggler AL, Mesecar AD, Van Breemen RB (2011) Modification of Keap1 cysteine residues by sulforaphane. Chem Res Toxicol 24:515–521. https://doi.org/10.1021/tx100389r
34. de Zeeuw D, Akizawa T, Audhya P, Bakris GL, Chin M, Christ-Schmidt H, Goldsberry A, Houser M, Krauth M, LambersHeerspink HJ, McMurray JJ, Meyer CJ, Parving H-H, Remuzzi G, Toto RD, Vaziri ND, Wanner C, Wittes J, Wrolstad D, Chertow GM (2013) Bardoxolone methyl in type 2 diabetes and stage 4 chronic kidney disease. N Engl J Med 369:2492–2503. https://doi.org/10.1056/nejmoa1306033
35. Hu L, Magesh S, Chen L, Wang L, Lewis TA, Chen Y, Khodier C, Inoyama D, Beamer LJ, Emge TJ, Shen J, Kerrigan JE, Kong ANT, Dandapani S, Palmer M, Schreiber SL, Munoz B (2013) Discovery of a small-molecule inhibitor and cellular probe of Keap1-Nrf2 protein-protein interaction. Bioorganic Med Chem Lett 23:3039–3043. https://doi.org/10.1016/j.bmcl.2013.03.013
36. Jiang Z-Y, Lu M-C, Xu L, Yang T-T, Xi M-Y, Xu X-L, Guo X-K, Zhang X-J, You Q-D, Sun H-P (2014) Discovery of potent Keap1–Nrf2 protein-protein interaction inhibitor based on molecular binding determinants analysis. J Med Chem 57:2736–2745. https://doi.org/10.1021/jm5000529
37. Wilson AJ, Kerns JK, Callahan JF, Moody CJ (2013) Keap calm, and carry on covalently. J Med Chem 56:7463–7476. https://doi.org/10.1021/jm400224q
38. Magesh S, Chen Y, Hu L (2012) Small molecule modulators of Keap1-Nrf2-ARE pathway as potential preventive and therapeutic agents. Med Res Rev 32:687–726. https://doi.org/10.1002/med.21257
39. Food and Drug Administration (FDA) (2016) Guidance for industry safety testing of drug metabolites guidance for industry, Guidance. Revision 1
40. Hetrick EM, Schoenfisch MH (2009) Analytical chemistry of nitric oxide. Annu Rev Anal Chem 2:409–433. https://doi.org/10.1146/annurev-anchem-060908-155146
41. Wallace JL (2005) Nitric oxide as a regulator of inflammatory processes. Mem Inst Oswaldo Cruz 100:5–9. https://doi.org/10.1590/S0074-02762005000900002
42. Franchi J, Marteau C, Crola Da Silva C, Mitterrand M, André P, Kieda C (2008) Cell model of inflammation. Biosci Rep 28:23. https://doi.org/10.1042/BSR20070012
43. Ashley NT, Weil ZM, Nelson RJ (2012) Inflammation: mechanisms, costs, and natural variation. Annu Rev Ecol Evol Syst 43:385–406. https://doi.org/10.1146/annurev-ecolsys-040212-092530


## Publisher's Note